Flow Boiling in Microgravity

G.P. Celata, G. Zummo

ENEA, Energy Department, Institute of Thermal Fluid Dynamics
Via Anguillarese 301, 00123 Santa Maria di Galeria, Rome, Italy; E-mail: celata@casaccia.enea.it

ABSTRACT

Flow boiling heat transfer (FBHT) can accommodate high heat transfer rates due to latent heat transportation. Its possible use is therefore potentially important to reduce size and weight of space platforms and satellites. A comprehensive knowledge is also important for the safe operation of existing single-phase systems in case of accidental increase of heat generation rate.

For space applications it is first necessary to identify the possible influence of microgravity conditions, and, in case of 'g' influence, evaluate the quantitative effect of reduced gravity on forced convective boiling heat transfer.

The number of existing researches on flow boiling in reduced gravity is very small due to large heat loads required and reduced available room in a 0-g apparatus for experiments, as well as complexity of the experimental facility for microgravity environment. As it can be expected, because of the reduced available data, coherence in existing data is missing.

This lecture will summarize the results of the few research carried out on FBHT in microgravity, with special emphasis to the recent research carried out at ENEA, in the frame of an ESA (European Space Agency) project.

INTRODUCTION

Flow boiling heat transfer is encountered in many engineering fields (energy conversion, environmental applications, food, chemical and other process industries, etc) and in space applications. In the coming years, expectations for space-based systems such as communication satellites and manned space-platforms or missions will grow rapidly. Due to the increasing size and capabilities of these systems, their power requirements will also greatly increase. More sophisticated thermal management systems capable of dealing with greater loads will have to be designed. FBHT may offer the solution for increasing heat transfer rates under future, challenging space conditions, at least under certain conditions and/or in certain areas of the system. High performance boiling heat transfer systems, which take advantage of the large latent heat transportation, are therefore important to reduce the size and weight of space platforms and satellites. Nonetheless, FBHT knowledge is also very important for the safe operation of existing single-phase liquid systems that may enter this mode of operation in case of accidental increase of the heat generation rate. An accurate understanding of the beyond-design situations is therefore essential for properly managing accidental situations.

Although the interest for FBHT systems in microgravity is high, the experimental research is still quite fragmentary and the knowledge of the physical phenomena involved is far from being complete. Most of phase change two-phase flow experiments performed were not responding to a phenomenological study purpose but to a more urgent need for engineering data such as the evaluation of International Space Station hardware, the stability of two-phase loops, flow regime evaluation and pressure drop measurements. While these experiments were relatively successful in providing a basic and partial understanding of those behaviours, the instrumentation has not yet reached the sophistication achieved in the environment of a typical terrestrial laboratory.

Among the available platforms for microgravity experiments, such as parabolic flight (gravity level 10^{-2}g, duration 20 s, repeated for about 30 times in a day), sounding rocket (gravity level 10^{-5}g, duration 2-15 min), orbital flight (gravity level 10^{-2}-10^{-5}g, duration unlimited), drop tower (gravity level 10^{-5}g, duration 2-10 s), because of the complexity of an experimental loop for flow boiling heat transfer tests the most widely used microgravity platform is the parabolic flight.

Due to limited availability of flight opportunities, the experimental activity in this area is still quite fragmentary and a general picture of the phenomena involved in flow boiling in microgravity is far to be completed, as already noted. However, some general conclusion may be drawn: i) results on heat transfer are contradictory, spanning form increase to decrease with respect to terrestrial gravity, and include no effect of gravity level; ii) the effect of gravity level on heat transfer strongly depends on the flow pattern; therefore, its knowledge is crucial and systematic visualisation tests are required; iii) forced convection flow (inertial effects) plays a fundamental role in microgravity flow boiling heat transfer as, added up to the buoyancy force, it may overcome it; the thresholds beyond which inertial effects are dominant over buoyancy effects have to be carefully determined; iv) a systematic study of flow boiling heat transfer is necessary in order to create a consistent data set for design purposes and to better establish the flow boiling heat transfer knowledge in microgravity.

The aim of the present paper is to provide with an overview of existing works along with a brief presentation of the results of a recent research in progress at ENEA, in the frame of an ESA (European Space Agency) project.

STATE-OF THE ART REVIEW

The few data available shows small coherence, maybe due to severe restrictions in the test apparatus specification, strict prescription of experimental conditions and not enough chance to repeat experiments for repeatability, short lasting of 0-g conditions, etc. A complete overview (including pool boiling) can be found in Ohta et al. [1], Ohta [2], Di Marco [3], Kim [4], and Ohta [5].

Saito et al. [6] reported heat transfer data of flow boiling of water in a horizontal annulus with a central heater rod during parabolic flight (about 22 s of microgravity conditions). Under microgravity condition, contrarily to terrestrial conditions where stratified flow often occurs unless you have high mass flux, bubbles are hardly detached from the heater rod due to the reduction of the buoyancy, flowing along the heater rod, and grow due to the heating by the heater rod and/or coalescence become much larger, surrounding the heater in the downstream. Tendency under microgravity was more noticeable in the cases of lower inlet fluid velocity, higher heat flux and lower inlet fluid subcooling. Results are shown in Fig. 1, where the fluid flow is from left to right. The differences of the local heat transfer coefficients are, however, very small in spite of large differences of the flow regimes under earth gravity and microgravity.

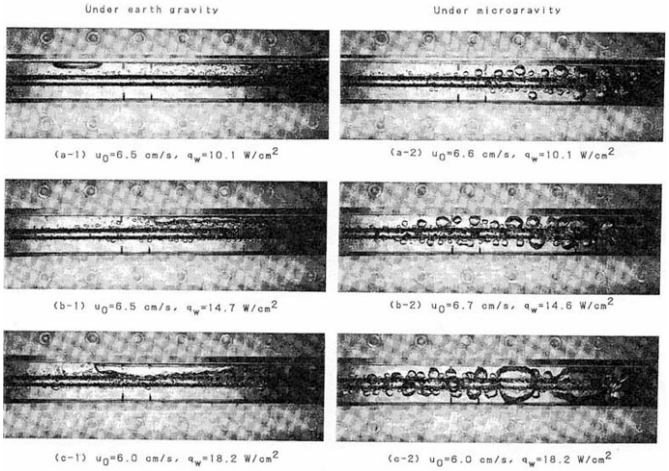

Fig. 1 - Typical pictures of bubble distribution at 1-g and 0-g in Saito et al. [6]

Lui et al. [7] carried out heat transfer experiments in subcooled flow boiling with R113 with a tubular tests section (12 mm i.d., 914.4 mm length). Subcooled boiling heat transfer was enhanced in microgravity conditions (parabolic flight). Heat transfer coefficients were approximately 5 to 20% higher in microgravity, generally increasing with higher qualities, as shown in Fig. 2. The greater movement of vapour bubbles on the heater surface caused more localised turbulence, which was believed to be responsible for the increased heat transfer coefficients.

Ohta et al. [8] and Ohta [9] studied flow boiling of R113 in a vertical transparent tube (8 mm i.d., 100 mm length), internally coated with a gold film, in parabolic flight. The flow rate ranged from 150 to 600 kg/m^2-s, and the heat flux from 2.5 to 80 W/m^2. Authors examined bubbly, slug and annular flow regimes. As usual, big variations in bubble and slug sizes with gravity level were observed. The heat transfer coefficient was barely affected by the various gravity levels provided that the heat transfer was controlled by nucleate boiling. As shown in Fig. 3, at low mass velocity a bubble detaching diameter decreases at 2-g, while it increases markedly at 0-g due to the reduction of buoyancy. The heat transfer dominated by nucleate boiling remains almost unchanged. At high mass velocity the bubble detachment is promoted by the shear force exerted by the bulk liquid flow and thus no marked change in the bubble behaviour and in the heat transfer is recognized with varying gravity level. At moderate quality, as shown in Fig. 4, where the annular flow pattern is observed regardless of gravity level, the nucleate boiling is completely suppressed as shown in the top Figure provided that heat flux is not so high. The heat transfer due to two-phase forced convection changes with gravity: it is enhanced at 2-g and is deteriorated at 0-g. At the same time, it is deduced from the increased transparency of the liquid film that the shear stress exerted on the film surface decreases at mg. At higher heat flux, the nucleate boiling occurs in the annular liquid film as shown in the bottom Figure. There is almost no effect of gravity on the nucleate boiling heat transfer as shown in the figure, where in the first half of the micro-g period the heat transfer deteriorated due to the frequent emergence of dry patches as a result of flow instability. In the case of low heat flux and high quality, it was confirmed that the effects of gravity on the behaviour of annular liquid film and thus on the heat transfer are decreased, because the effect of shear force exerted by the vapour core flow with increased velocity exceeds that of the gravitational force on the behaviour of annular liquid film.

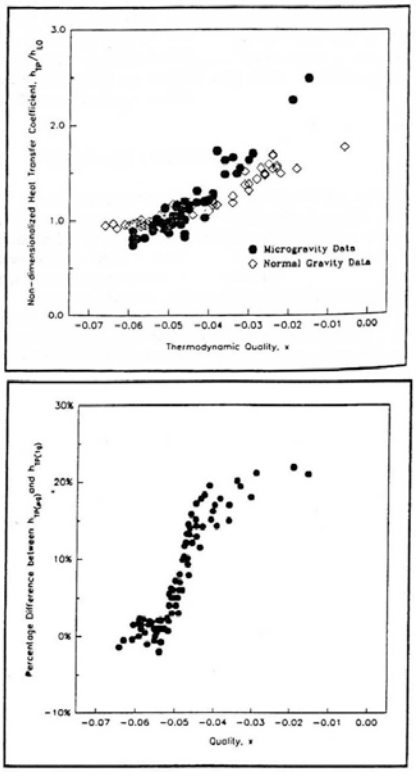

Fig. 2 – Non-dimensional heat transfer coefficient (top) and percentage difference between 1-g and 0-g conditions (bottom) in Lui et al.[7]

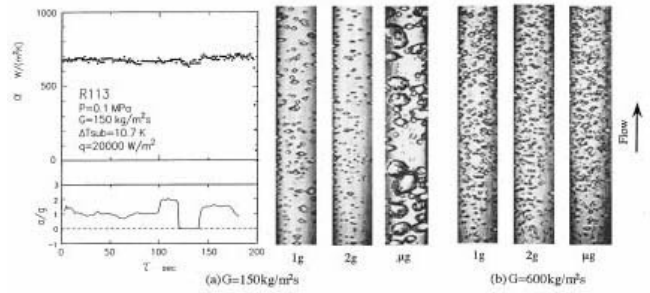

Fig. 3 – Visualization of boiling heat transfer (low quality) in Ohta et al. [9]

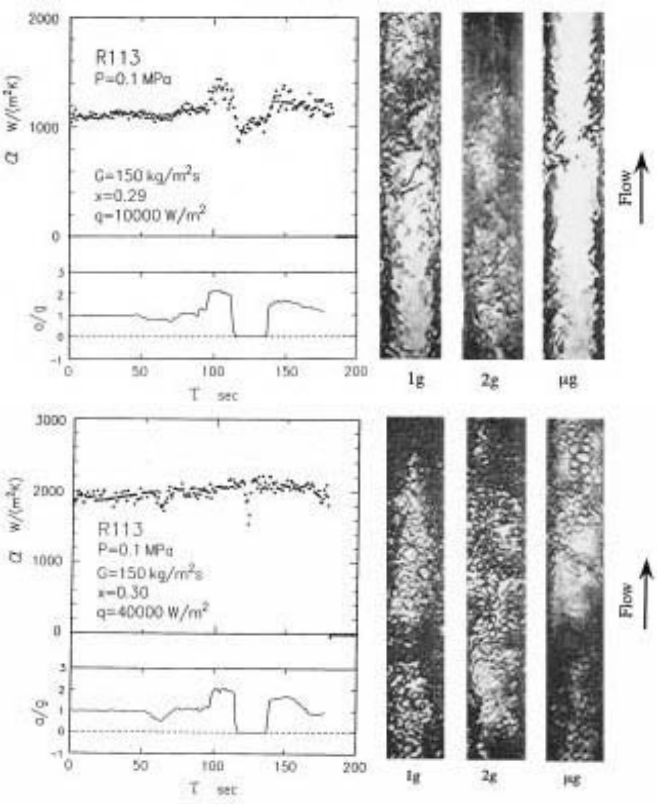

Fig. 4 – Visualization of boiling heat transfer (medium-high quality) in Ohta et al. [9]

Ma and Chung [10, 11] performed forced-convection boiling of FC-72 in normal gravity and microgravity conditions (drop tower, 1 s of microgravity conditions) using a uniformly heated flat square plate as test section. They obtained boiling curves and flow maps for different flow rates in microgravity. It was observed that the forced flow decreased the average bubble size and kept boiling in the nucleate boiling regime in microgravity. With the increase in flow rate, the heat transfer coefficient increased while average superheat of the heater surface decreased. They found that forced convection also enhances the departure of bubbles from their nucleation sites. It was noted that for high heat flux curves, no matter whether in terrestrial gravity or in microgravity, the curves tend to be close together as Reynolds numbers increase. For Reynolds number > 10.000, no influence of gravity has been found. Results are shown in Fig. 5, where the bubble growth is plotted as a function of the flow rate in terms of non-dimensional detachment diameter (D* = D/La, with La Laplace length) and non dimensional volume, V*, with increasing heat flux (top) and increasing (non-dimensional) time, t* (bottom). Figure 6 shows the effect of forced convection on bubble generation frequency, for a given heat flux.

An interesting experiment of flow boiling visualization has been carried out by Westheimer and Peterson (2001), who used a glass annular heat exchanger, and R-113 as fluid, in parabolic flight. Results from this work illustrated the following trends: 1) less heat addition was needed to cause flow regime transitions in reduced gravity environments; 2) Earth-based flow regime maps did not correlate well with visual data or 0-g flow regime maps; 3) all of the 0-g flow regime maps produced similar results for calculations of quality, heat-transfer coefficient, and heat-exchanger temperature, indicating that all of them were acceptable for this application; and 4) that maximum heat transfer occurred at locations in the heat exchanger near the transition from bubble to slug flow. Typical video frames data of the experiment are reported in Fig. 7a, 1.8-g manoeuvre, and Fig. 7b, which shows the same portion of the test section a few seconds later while in reduced gravity. During 1.8-g conditions primarily small bubbles and a chaotic churn flow were found in the test section, while slug flow was almost nonexistent, probably because of a combination of fluid properties and heating conditions. Figure 7 clearly show that by decreasing the gravitational acceleration and maintaining the other test conditions nearly constant the bubbles grew larger and bubble, slug, and annular flow regimes were clearly present. Another observation that these pictures cannot illustrate was that the bubble speed drastically decreased as the test conditions approached reduced gravity. Decreased bubble speed in reduced gravity illustrated the effect of buoyancy on the dynamics of the vapour bubbles. Figure 7b illustrates that frothy annular flow was seen in reduced gravity environments. It appears that the frothy annular flow was very similar to churn flow, especially when the trend of larger bubbles in reduced gravity is considered.

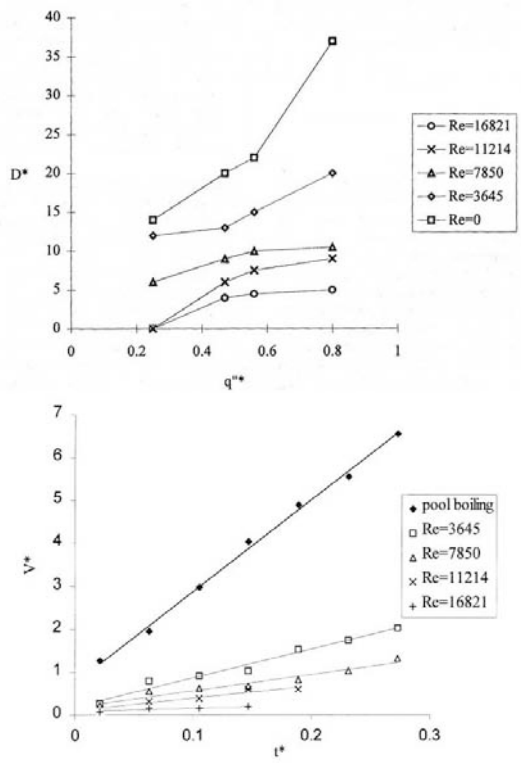

Fig. 5 - Forced convection effect on average bubble size with increasing heat flux (top, Ma and Chung, [10]) and bubble volume for a given heat flux (bottom, Ma and Chung, [11])

As far as the critical heat flux (CHF) is concerned, even less results are available, because of the more difficult conduction of the experiment in the frame of the few seconds available in microgravity environment (parabolic flight and drop tower).

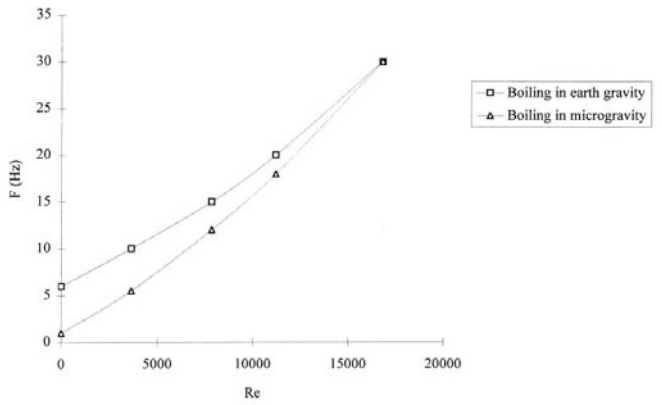

Fig. 6 - The effect of forced convection on bubble generation frequency, for a given heat flux, Ma and Chung [11]

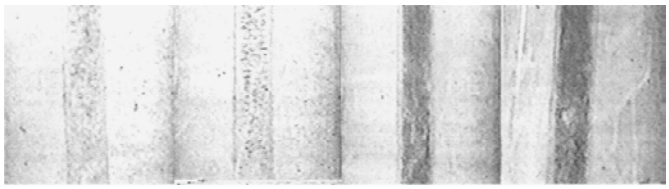

Fig. 7a – Visual data, 1.8-g, Westheimer and Peterson [12]

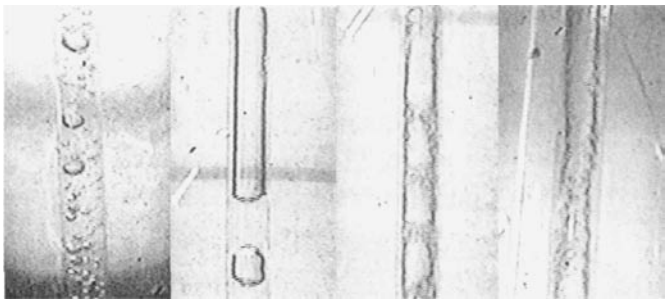

Fig. 7b – Visual data, 0-g, Westheimer and Peterson [12]

Ohta and co-workers (above references) have conducted few experiments, finding that CHF is independent of the gravity level as the fluid flow rate is increasing above a critical value (depending on channel size, thermal-hydraulic conditions, etc.).

Ma and Chung [13] using the same experimental apparatus described in Ma and Chung [10, 11], performed an experiment of CHF in a drop tower test (2.1 s of microgravity conditions). The CHF in microgravity is lower than that in terrestrial gravity, but, when the flow rate is increased, the two lines tend to approach each other. This phenomenon suggests that the CHF values in terrestrial gravity and microgravity would be similar in magnitude if the flow rate reaches a certain value. Results are plotted in Fig. 8, where the critical heat flux is plotted versus the Reynolds number (fluid flow velocity) for microgravity and terrestrial gravity conditions.

Very recently Zhang et al. [14] carried out an experiment of CHF in a rectangular duct channel on a parabolic flight using FC-72 as process fluid. The found that CHF in microgravity at low velocities is significantly smaller than in horizontal flow at terrestrial gravity. The difference in CHF magnitude between the two environments decreases with increasing velocity, culminating in a virtual convergence of microgravity and terrestrial gravity data at 1.5 m/s for FC-72. Such a result is shown in pictures of Fig. 9, where higher liquid velocities greatly dampened the effects of gravity. This proves it is possible to design inertia-dominated space systems by maintaining flow velocities above the convergence limit. Such inertia-dominated systems allow data, correlations, and/or models developed on ground to be safely implemented in space systems.

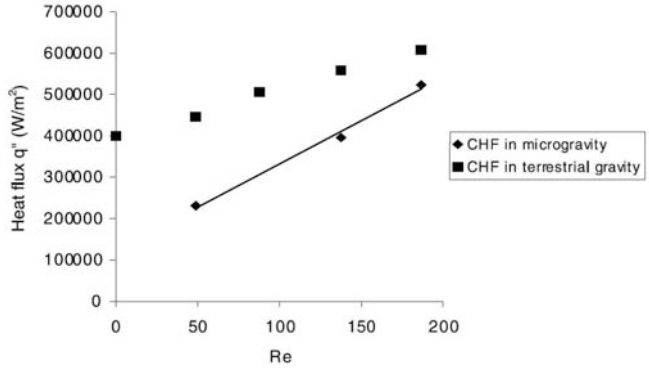

Fig. 8 - The effect of forced convection on critical heat flux, Ma and Chung [13]

Antar and Collins [15] obtained flow pattern visualization and wall temperature measurements during quenching of hot tube aboard the NASA KC-135 aircraft, using saturated liquid nitrogen. Two test sections are used, 10.5 mm i.d. and 600 mm in length, and 4.32 mm i.d. and 700 mm in length. Authors describe a new two-phase flow pattern at reduced gravity indicated as *filamentary flow*. The filamentary flow is a sort of inverted annular flow characterised by a long liquid filaments flowing in the centre of the channel and surrounded by vapour. The filaments have a diameter of approximately one third of the pipe diameter. Rewetting time is found to be longer than that at normal gravity (lower rewetting velocity).

Westbye et al. [16] performed quenching experiments of hot tube aboard the NASA KC-135 using subcooled R113 in a horizontal stainless steel tube, 11.3 mm i.d. and 914 mm in length. Rewetting temperature at low gravity is 15-25 °C lower than at normal gravity. Heat transfer coefficients during film boiling at low gravity are lower (up to 50%) than those at normal gravity. Therefore, the total duration of quenching process is found significantly longer at microgravity (lower rewetting velocity). The observed flow pattern at μ–g is inverted annular flow and dispersed flow, with a thicker vapour film thickness in inverted annular flow.

In spite of the available results there are still important un-answered questions which still are looking for an answer:

- ✓ Is boiling heat transfer in 0-g enhanced or deteriorated with regard to ground tests?
- ✓ What is the flow conditions threshold for which 0-g does not affect flow boiling heat transfer? (inertial effects are dominant over buoyancy)
- ✓ What about the CHF?

Indeed, some experimental results show enhancement of heat transfer in 0-g, while others show deterioration or negligible effect of gravity level on boiling heat transfer. Also, though some experimental results show thresholds in gravity level

influence on flow boiling heat transfer, they are leopard spot like and do not allow any clear conclusion. Systematic findings in these areas will make design of flow boiling heat transfer systems for space applications possible in a more reliable way.

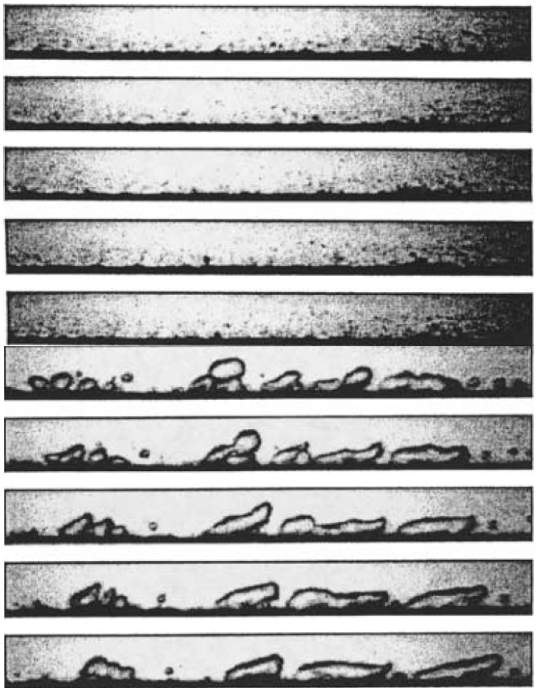

Fig. 9a – Pictures taken at 0.14 m/sat, during terrestrial gravity (top) and microgravity conditions, CHF (bottom), Zhang et al. [14]

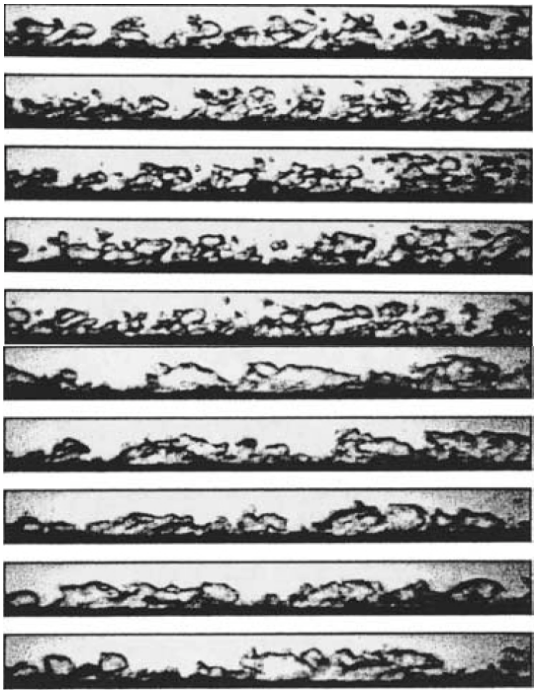

Fig. 9b - Pictures taken at 1.4 m/sat terrestrial gravity (top) and microgravity conditions, CHF (bottom), Zhang et al. [14]

ESA, the European Space Agency, has recently funded some projects on flow boiling. In this frame, ENEA is supposed to perform a large number of tests on parabolic flights in order to gather a consistent data set of boiling heat transfer, flow pattern bubble dynamics and CHF.

THE ENEA RESEARCH

The activity is carried out on the experimental facility called MICROBO (MICROgravity BOiling), specifically designed and built to be boarded on the Airbus A300 ZERO-Gravity managed by Novespace for parabolic flight experiments of ESA, French and German Space Agencies. A schematic of the facility is drawn in Fig. 10, while Fig. 11 shows a picture and a sketch of wall thermocouple position for the test section use in the experiment. The maximum flow rate is 500 ml/min, while the maximum pressure is 6 bar obtained with nitrogen and reduced to about 2 bar for tests with Pyrex test sections. The maximum wall temperature (pier tube) is 230 °C, while the maximum temperature of FC-72 (the process fluid) is 90 °C. Available thermal power on the aircraft is 150 W for the electric pre-heater and 180 W for the test section.

A typical test section in Pyrex is shown in Fig. 10 The inner diameter is 6.0 mm (thickness is 1.5 mm) and the heated length is 165 mm. The fluid is heated by the electrical tape helically twisted on the external surface of the pipe. The test section is placed vertically and the flow is upward. Additional Pyrex test sections of 4 and 2 mm i.d. are used in the project.

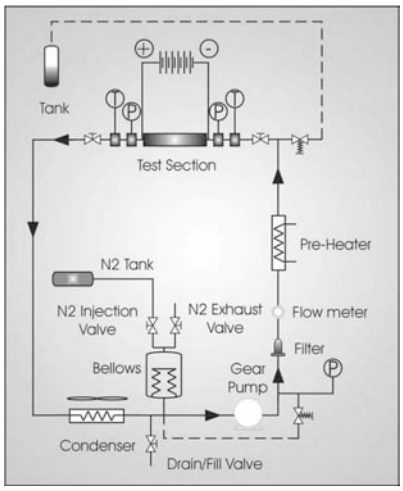

Fig. 10 – Schematic of the MICROBO facility

Fig. 11 – Picture of the test section used in the MICROBO loop

THE ENEA EXPERIMENTAL RESULTS

ENEA already carried out five experimental campaigns, starting in October 2004, where flow visualization, boiling heat transfer and quenching tests have been performed. An experimental campaign in parabolic flight consists in three days flight, where about 30 parabolas are performed each day, where conditions of 10^{-2} g are obtained for about 22 s in each parabola. Under microgravity conditions, apart from possible coalescence, the size of a bubble depends basically on its diameter at the detachment. This latter, in flow boiling, depends on the forces balance, where the most important are the surface tension (adhesive force), the buoyancy and the drag forces (dislodging forces). Of course, under microgravity conditions where the buoyancy force is missing,

the detachment bubble diameter tends to be generally larger than at terrestrial gravity (other conditions being equal), unless the fluid velocity is so high that buoyancy force can be negligible even at 1-g. This complex balance will also depend on system pressure (which affects the bubble size), heat flux (coalescence effects) and diameter size (which affects the flow pattern). The size of the bubble will affect the thermal hydraulics in flow pattern, pressure drop and heat transfer. The knowledge of the limits of the influence of gravity level is of fundamental importance in the design of two-phase systems for space applications.

Flow Rate Influence on Gravity Effect in Heat Transfer

Figures 12 and 13 show the trend of some wall thermocouples during one parabola, i.e., for different gravity levels, for a velocity of 3 cm/s and 30 cm/s, respectively. Thermal hydraulic conditions are specified in the figure captions. Before and after the microgravity region (~22 s) we have two time spans of about 20 s where the gravity level is about 1.8 g. This happens in the first ascending part and in the last descending part of the parabola. With reference to Fig. 12 (low fluid velocity, 3 cm/s) the three wall thermocouples have an almost constant trend in 1-g and 1.8-g conditions, while the wall temperature tends to increase and then to stabilize around a higher value indicating a reduction of the heat transfer coefficient (heat flux and system pressure are practically constant). In the 1.8-g level after the microgravity period the wall thermocouples fall down the value they had before the parabola (effect due to bubbles collapse). Looking at Fig. 13, where the fluid velocity is about 30 cm/s, i.e., ten times higher, it is possible to see how wall thermocouples are almost stable (heat transfer independent of g-level) for the whole parabola. The two tests refer to an almost constant low quality. Under these conditions, and for the 6.0 mm test section the influence of gravity level disappear when the fluid velocity is higher than 25 cm/s.

Vapour Quality Influence on Gravity Effect in Heat Transfer

As the possible influence of gravity on the heat transfer depends also on vapour quality, some tests have been conducted with different qualities values for similar fluid velocity, to ascertain its possible influence. The test reported in Fig. 14 is characterized by same conditions of the test reported in Fig. 12 but with a higher heat flux (23 kW/m^2) and, correspondingly, a higher vapour quality, 0.3. Under these quality conditions even for very low fluid velocity the heat transfer is practically unaffected by the gravity level. We may reasonably affirm that for a quality above 0.3 the gravity effect is negligible independent of the fluid velocity.

Inter-Relation Between Fluid Velocity and Quality on Gravity Effect in Heat Transfer

As the gravity effect on heat transfer may depend both on fluid velocity and vapour quality, it is quite important to have a global representation of the gravity influence as a function of these two parameters. This has been attempted, though preliminarily, in a non-dimensional term in Fig. 15, where the Reynolds number, Re, is plotted as a function of vapour quality, x. All experimental data obtained for the 6 and 4 mm pipe have been plotted in this graph, where the curve which separates the region of gravity influence from that of no influence is drawn.

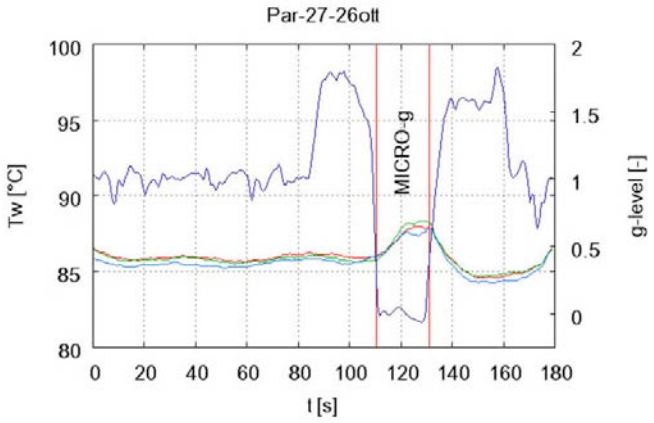

Fig. 12 – Typical wall temperature trace as a function of gravity level and low flow rate (G = 47.5 kg/m^{2}s, ~ 3 cm/s; q" = 10200 W/m^2, x = -0.05, p_{out} = 0.18 MPa, ΔT_{in} = 25 K)

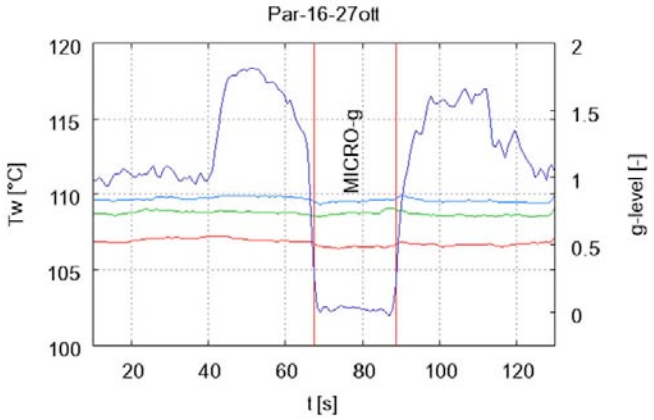

Fig. 13 – Typical wall temperature trace for different gravity levels and high flow rate (G = 439 kg/m^{2}s, ~ 30 cm/s; q" = 37400 W/m^2, x = -0.08, p_{out} = 0.16 MPa, ΔT_{in} = 15 K)

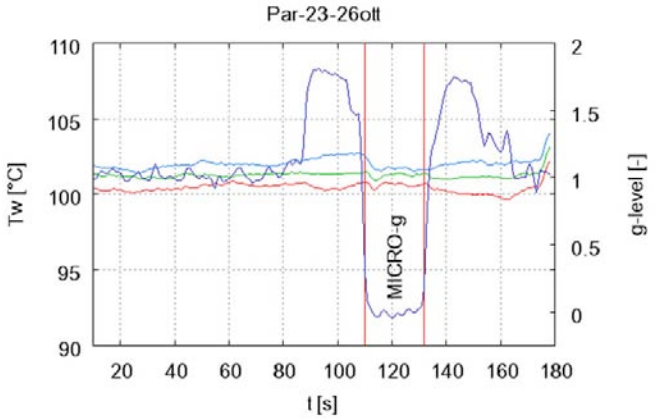

Fig. 14 – Typical wall temperature trace as a function of gravity level, for low flow rate and high vapour quality (G = 47.5 kg/m^{2}s, ~ 3 cm/s; q" = 23000 W/m^2, x = 0.3, p_{out} = 0.18 MPa, ΔT_{in} = 25 K)

Gravity Level Effect on Bubble Size and Flow Pattern

It has been already said about the possible influence bubble size and distribution on the heat transfer. It is therefore reasonable to expect a larger bubble size wherever we have a clear difference in heat transfer, while when the

heat transfer is practically not affected by gravity we may expect similar bubble size and distribution.

Figure 16 shows two pictures extracted from high-speed movies taken during parabolic flights, the top figure referring to 1-g conditions and the bottom one to 0-g conditions, for the 6 mm i.d. pipe. Thermal hydraulic conditions are of low flow velocity ad low quality. Under these conditions the heat transfer is affected by the gravity level and bubble size in microgravity is definitely larger than at 1-g.

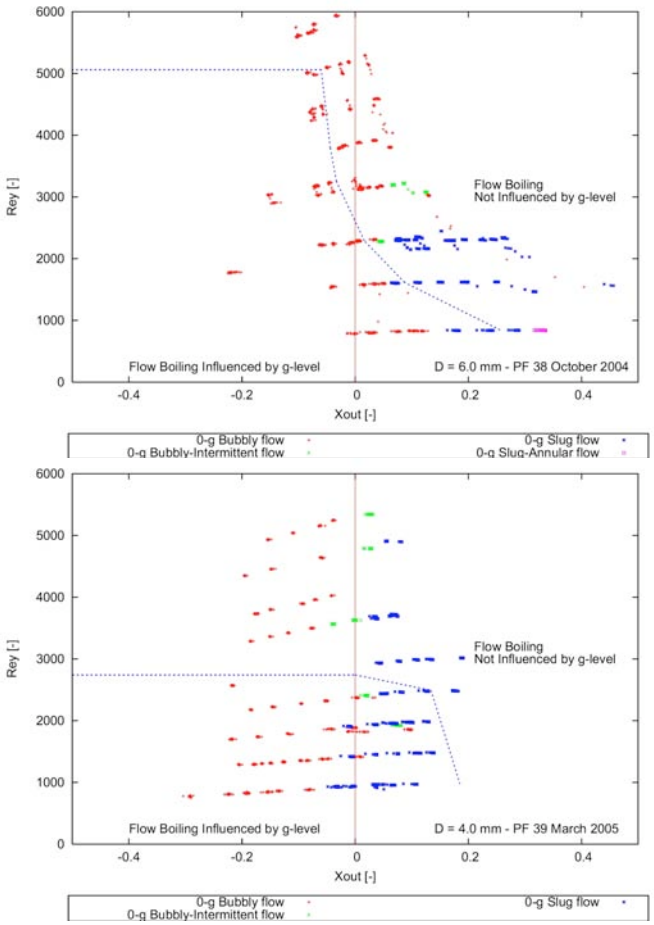

Fig. 15 – 0-g map for the inter-relation between fluid velocity and quality on gravity effect in heat transfer, D = 6 mm (top) and D = 4 mm (bottom)

Increasing the fluid velocity, other conditions being equal, beyond the limit of gravity influence on heat transfer, one may observe how bubble size is practically similar for 1-g and 0-g conditions. A typical example is reported in Fig. 17 where, similarly to Fig. 16, 1-g conditions (top figure) are compared with 0-g condition (bottom figure).

Similarly, for the 4 mm i.d. pipe, we can see how in bubbly flow at low mass flux and heat flux there is a large influence of the gravity level on the shape of bubbles Always for tests with D = 4 mm i.d. pipe, for higher mass flow fluxes, the differences of flow patterns in bubbly and intermittent flow are less important, as shown in Figs. 19 and 20. Figures 19 and 20 show the bubbly flow and intermittent annular flow at 1-g (top) and 0-g (bottom), for the same inlet conditions: G = 355 kg/m^2-s, $\Delta T_{sub,in}$ = -25.3 K, and p = 1.8 bar, but different heat fluxes. Qualitatively, the bubbly flow pictures of Figure 19, show minimal differences, vapour bubble dimensions are very similar. In the pictures of Figure 20, where an annular flow regime is depicted, geometry and shape of the flow pattern at 1-g (top) and 0-g (bottom) look very similar.

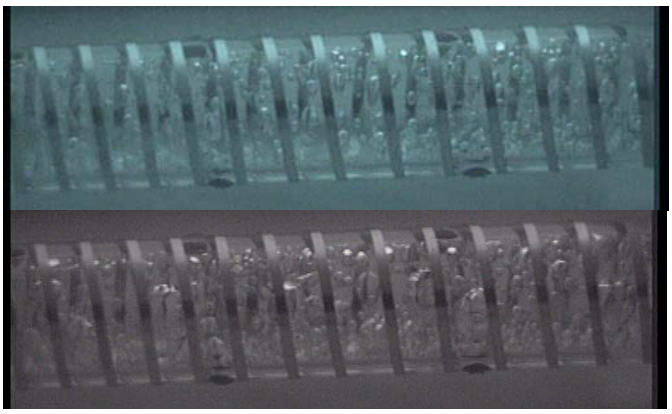

Fig. 16 – Flow pattern at 1-g (top) and 0-g (bottom) for low fluid velocity and low quality (G = 96 kg/m^{2}s, ~ 6.4 cm/s, q" = 22660 W/m^2, x = -0.06, p_{out} = 0.18 MPa, ΔT_{in} = 27.5 K), D = 6 mm

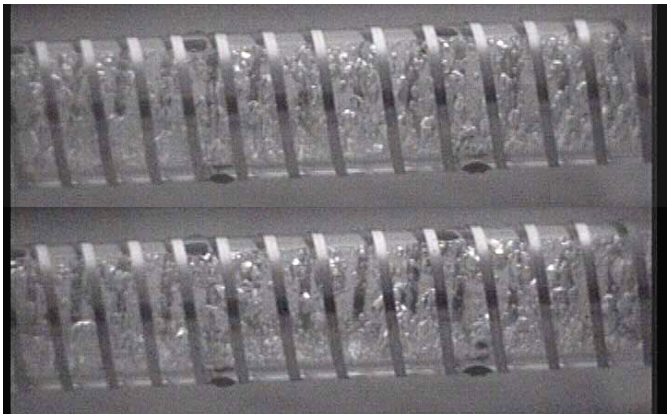

Fig. 17 – Flow pattern at 1-g (top) and 0-g (bottom) for high fluid velocity and low quality (G = 439 kg/m^{2}s,~ 30 cm/s, q" = 37400 W/m^2, x = -0.08, p_{out} = 0.16 MPa, ΔT_{in} = 15 K), D = 6 mm

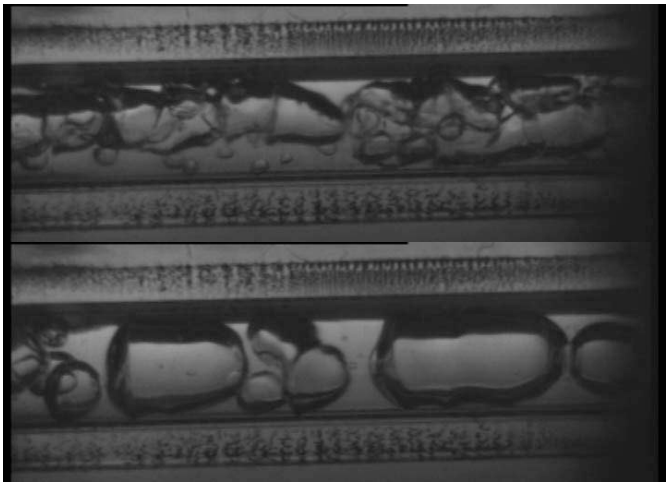

Fig. 18 – Flow pattern at 1-g, top, and 0-g, bottom, q" = 23800 W/m^2, x_{out} = 0.066, D = 4 mm (low mass flux)

Fig. 19 – Flow pattern at 1-g, top, and 0-g, bottom, G = 355 kg/m^2-s, $\Delta T_{sub,in}$ = -25.3 K, and p = 1.8 bar, D = 4 mm (intermediate heat flux)

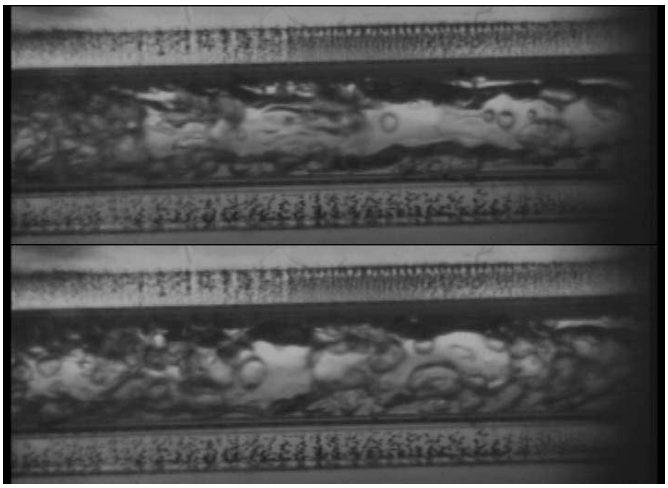

Fig. 20 – Flow pattern at 1-g, top, and 0-g, bottom, G = 355 kg/m^2-s, $\Delta T_{sub,in}$ = -25.3 K, and p = 1.8 bar, D = 4 mm (high heat flux)

Flow Pattern Maps

Typical experimental flow pattern data for microgravity tests (4.0 mm tube) are plotted in fig. 21 as a function of exit quality and mass flow-rate. For subcooled flow boiling, where the exit thermodynamic quality is negative, the typical flow pattern is of the bubbly flow type.

Bubbly flow is also observed in the saturated flow boiling region, but only in the near zero quality area, for exit quality ranging from 0.0 up to 0.04. In the saturated flow boiling region, for increasing values of quality, flow pattern becomes of the intermittent flow type. Two types of intermittent flow are observed: plug flow and a more disordered intermittent flow. The graph clearly shows that plug flow is observed for mass flow-rates lower than 230 kg/m^2-s. For higher values of mass flow-rate, the flow pattern gradually becomes of the disordered intermittent flow type.

Typical experimental flow pattern data for microgravity tests (6.0 mm tube) are plotted in fig. 22 as a function of exit quality and mass flow-rate. Bubbly flow is observed also in the saturated flow boiling region, but only in the near zero quality area, for exit quality ranging from 0.0 up to 0.1. In the saturated boiling region, for increasing values of quality, flow pattern becomes of the intermittent flow type. At high mass flow-rate, due to the restrictions on electrical power, only bubbly flow points were obtained during parabolic flights.

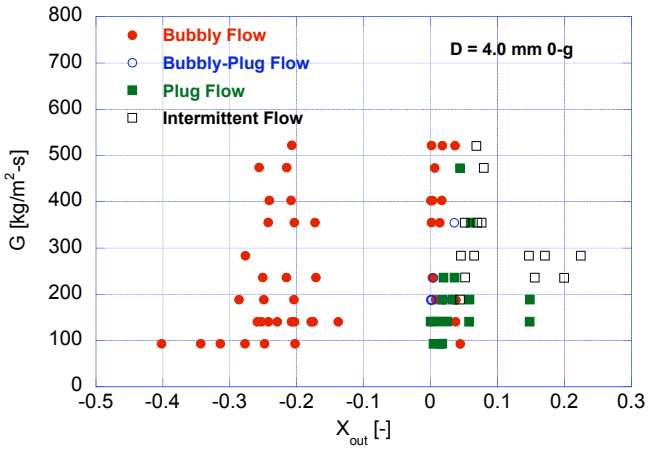

Fig. 21 – Microgravity flow pattern data for the 4.0 mm tube

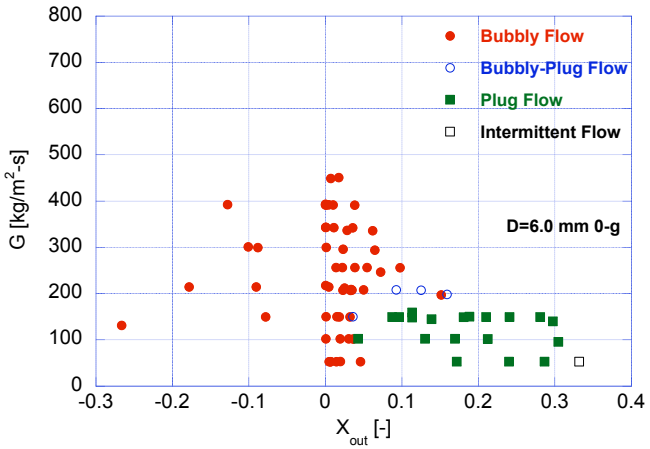

Fig. 22 – Microgravity flow pattern data for the 6.0 mm tube

As far as the possibility to predict experimental flow pattern data using maps is concerned, among the few available (Celata et al. [17]) the best prediction (though not accurate) has been provided by the map proposed by Dukler and his colleagues (Colin et al. [18], and Dukler et al. [19]). They developed a flow pattern map for microgravity conditions (and gas-liquid flow), identifying three kind of flow pattern under microgravity: bubbly flow, slug flow, and annular flow, and tested the proposed map with a microgravity dataset (always gas-liquid flow data). The transition from bubbly to slug flow occurs due to the coalescence of bubbles when the bubble concentration reaches a certain value. Authors propose this transition as occurring for a void fraction value of 0.45. Besides, they observe that the local relative velocity between liquid and gas is negligible, thus confirming the expected equivalence between liquid and gas velocity in microgravity (i.e., no-slip condition, u_G/u_L = 1). From the no-slip condition, starting from the definition of liquid and vapour superficial velocities we can write:

$$\frac{j_L}{j_G} = \frac{1-\alpha}{\alpha} \qquad (1)$$

As the transition from bubbly to slug flow is postulated to occur when $\alpha = 0.45$, eq. (1) yields:

$$j_L = 1.22\, j_G \qquad (2)$$

According to this model the bubbly to slug flow transition is independent of tube diameter.

The transition from slug to annular flow occurs when the two void fraction values, calculated for slug flow and annular flow with two different models, reach the same value. However, no annular flow conditions have been experienced in our research.

The transition lines, calculated with the previous equations (1) and (2), are compared in the graph of fig. 23 with the experimental observations of the 4.0 mm tube data. The observed flow pattern is bubbly and intermittent flow (plug or slug). Some of the bubbly flow points fall in the slug flow region, while almost all intermittent flow data points are in the slug flow region.

The experimental results obtained with the 6.0 mm diameter tube are plotted in the graph of fig. 24. This graph shows many bubbly flow data points falling outside the bubbly flow region predicted by the map, while the slug flow data points are predicted mostly in the slug flow region.

In both figures 23 and 24 we have also plotted in the graph a dashed line which represents the transition from bubbly to intermittent flow when the void fraction reaches the threshold value of 0.74. The origin of this particular value of void fraction comes from the sphere packing theory which concerns arrangements of non-overlapping identical spheres filling a volume. When the void fraction of a bubbly flow exceeds this limit value, the bubble packing is so dense that coalescence of small bubbles into a larger one is highly probable and the formation of Taylor bubbles occurs in the flow channel. Dukler proposed $\alpha = 0.45$ as the void fraction value at the transition between bubbly and slug flow. This value was the mean value obtained from the void fraction of spheres in a cubic array (0.52) and the void fraction of ellipsoids (0.40). According to the so-called Kleper conjecture (see Weisstein [20-21]), the densest possible packing of rigid spheres with the same radius arranged in a cubic close packing is

$$\beta = \frac{\pi}{3\sqrt{2}} = 0.74048 \qquad (3)$$

where β is the packing density, i.e., the fraction of a volume filled by solid spheres. If solid spheres are replaced by small vapour bubbles the packing density is equal to the local volumetric void fraction. When the slip ratio, $s = u_G/u_L$ is equal to 1, as in the case of microgravity two-phase flows, the volumetric void fraction is coincident with the cross sectional void fraction α. Therefore, it is possible to consider 0.74 as the largest value of void fraction of packed small vapour bubbles in bubbly flow. This is the limit at which coalescence occurs and slug flow takes place in the flow channel. The bubbly-intermittent flow transition calculated with $\alpha = 0.74$ shows a better agreement with the experimental data for 6.0 mm tube, especially for lower mass flow-rate data characterized by a liquid superficial velocity, j_L, lower than 0.1 m/s. However, for j_L higher than 0.1 m/s some bubbly flow data points are located inside the slug flow region, but very close to the transition line. The graph shows, also, that all the intermittent flow data points lie to the right of this modified boundary line. Some of the intermittent flow data points are placed in the annular flow region, but close to the boundary line.

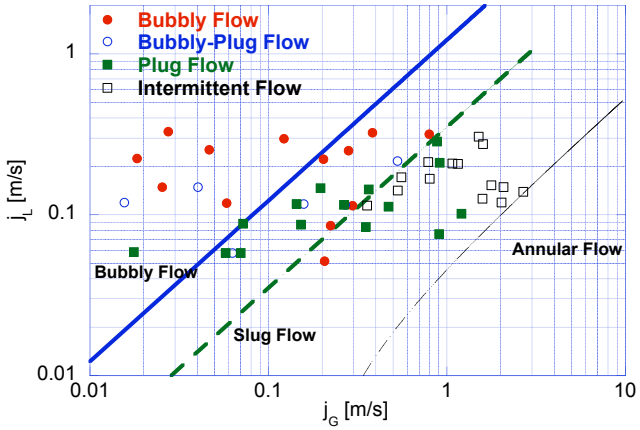

Fig. 23 - Dukler et al. [19] flow pattern map for microgravity data (4.0 mm tube)

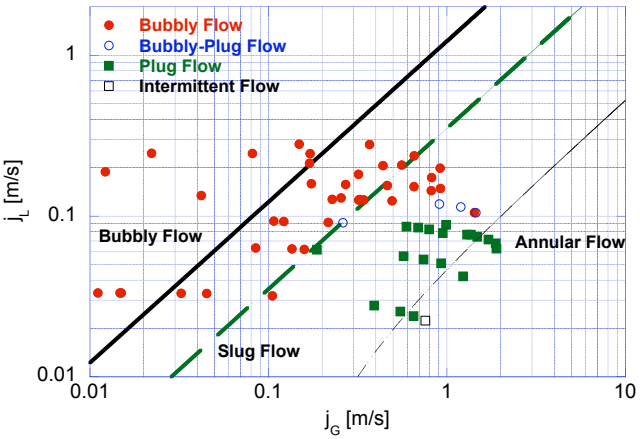

Fig. 24 - Dukler et al. [19]) flow pattern map for microgravity data (6.0 mm tube)

Results plotted in figs. 23 and 24 would seem to suggests that the tube diameter plays a role which is not taken into the account in eq. (2).

Quenching

At the beginning of the quenching experiments, when the liquid is injected in the hot tube, only a stream of vapour is in contact with the channel wall. Vapour heat transfer is not very effective but, as the thermal power is switched off, a first reduction in the wall temperature is observed, after the peak value. In this phase, the heat transfer regime is governed by film boiling, and the liquid cannot touch the hot wall due to its high temperature. When the wall temperature is reduced to the rewetting temperature, the liquid is able to come into direct contact with the channel walls and nucleate boiling occurs. At this time the heat transfer rate from the hot wall to the liquid is significantly increased and a rapid variation of the wall temperature slope can be observed.

The quenching (or rewetting) temperature is defined as the temperature obtained by drawing the tangents on the transient temperature curves in the regions where the significant change of the curve slope occurs, as schematically drawn in Fig. 25, which represents a typical plot of a

quenching curve for one wall thermocouple. In this figure, the rewetting temperature, T_{rew}, and rewetting time, t_{rew}, are plotted with reference to the thermocouple T_{w3} (dotted line). This procedure is used for all thermocouples readings which exhibit the characteristic significant change in their slope.

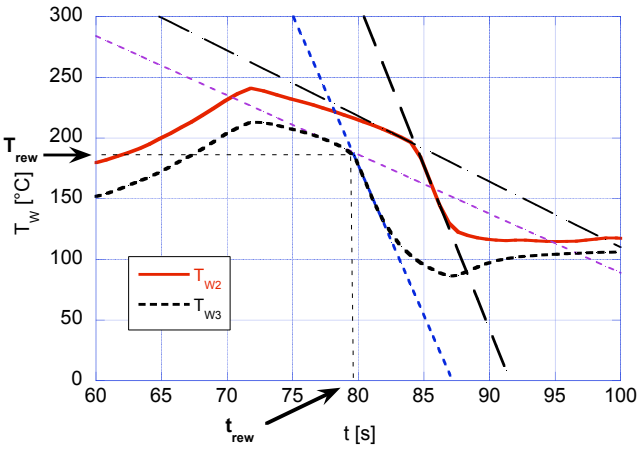

Fig. 25 - Method for the determination of the rewetting temperature and time; values indicated on the axes refer to the dotted line wall temperature

The results of the rewetting velocity as a function of mass flux for terrestrial and reduced gravity are shown in Fig. 26 for the D = 2.0 mm pipe. The rewetting velocity indicates the speed at which the quench front moves from the inlet along the hot tube, and is the responsible of the time necessary for the rewetting of the whole tube. Generally, the quench front velocity is significantly lower, often an order of magnitude lower, than the liquid velocity. In fact, for the 2.0 mm tube diameter, the maximum liquid velocity is 0.25 m/s, while the highest quench front velocity is about 4 mm/s. Figure 26 clearly shows that the rewetting velocity in microgravity is lower than that at normal gravity, other conditions being equal, the difference being more evident as the mass flux increases. As a general trend, the quench front velocity at terrestrial gravity is a continuous increasing function of mass flux. In turn, at microgravity conditions it appears to be almost independent of mass flux, resulting lower than at terrestrial gravity as mass flux increases.

Figures 27 and 28 show the plot of the quench front velocity as a function of mass flux for the other two tested tubes, i.e., 4.0 and 6.0 mm pipe. The intermediate diameter, D = 4.0 mm (Fig. 27), shows some data scatter, but the quench front velocity would not seem seems to be affected by the gravity level, at least within the experimental uncertainty. Unfortunately, these tests have been carried out under strong turbulence during the low gravity period, and gravity level never went below 0.4g. So, any conclusion on these data is not properly referring to microgravity conditions, at least to the gravity level of the other two pipe diameters.

Data for D = 6.0 mm tube diameter are plotted in Fig. 28 and shows that the rewetting velocity at reduced gravity is much lower than that at normal gravity, other conditions being equal, reducing to even one third of the terrestrial gravity value. Again we have that the quenching velocity in microgravity looks almost independent of G, while it increases with G at terrestrial gravity.

As far as the tube diameter is concerned we may state that the quench front velocity would seem to be affected by the channel size. The quench front velocity appears to be an increasing function of the pipe diameter, conclusion which is valid both for microgravity and terrestrial gravity conditions.

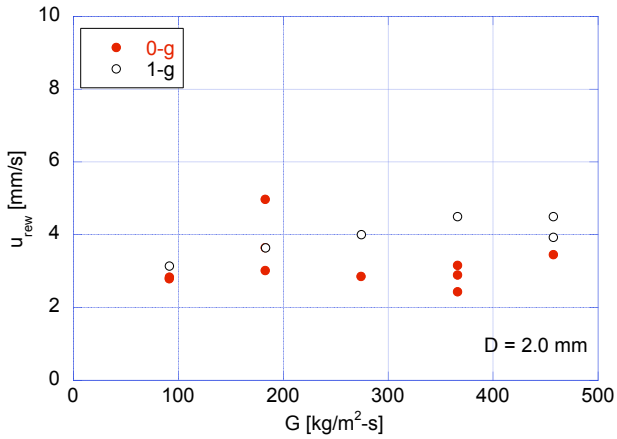

Fig. 26 - Rewetting velocity versus mass flux for 1-g and 0-g test (D = 2.0 mm)

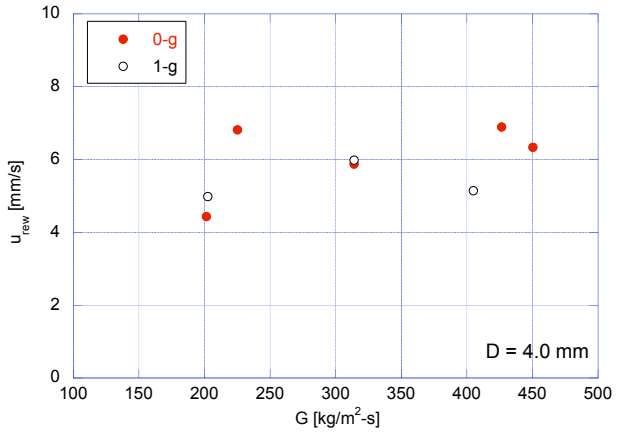

Fig. 27 - Rewetting velocity versus mass flux for 1-g and 0-g tests (D = 4.0 mm)

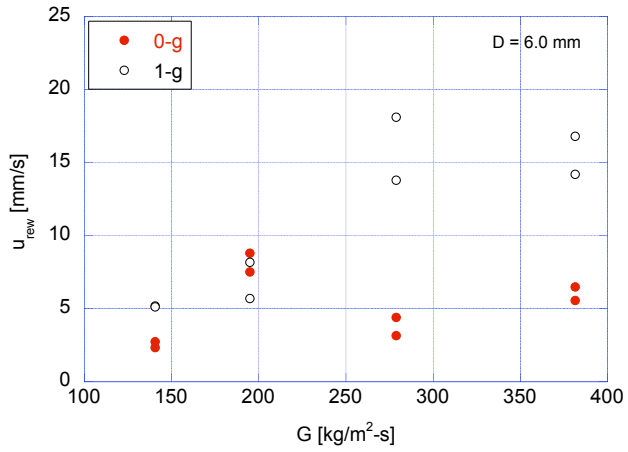

Fig. 28 - Rewetting velocity versus mass flux for 1-g and 0-g tests (D = 6.0 mm)

As a general conclusion we may say that the microgravity influence is higher for larger diameter pipe. Further experimental campaigns are therefore needed to have a better physical insight in quenching at microgravity conditions.

CONCUDING REMARKS

Flow boiling heat transfer in microgravity has received relatively little attention so far due to complexity of the experiment, large heat loads and available room in a 0-g apparatus for experiments. Therefore, the few experiments available, which are summarized in the present paper, are sparse and sometimes exhibit contradictory findings: heat transfer has been found higher or lower than at terrestrial gravity without apparent explanation. Sometimes, the short duration of microgravity conditions does not allow a full development of flow boiling heat transfer, thus spoiling the experimental evidence.

After e review of available experimental results, the program of ESA projects on flow boiling research is briefly highlighted, and results of some experimental campaigns carried out on parabolic flights are also briefly reported.

Generally, microgravity conditions lead to a larger bubble size which is accompanied by a deterioration in the heat transfer rate. The influence of gravity level on heat transfer tends to decrease as the fluid velocity increases, also depending on vapour quality. For low quality, gravity influence can be considered negligible when the fluid velocity is greater than 25 cm/s. For quality larger than 30%, no influence of the gravity level is observed independent of the fluid velocity. The inter-relation between fluid velocity and vapour quality has been quantified.

Observed flow pattern at low gravity is: bubbly, plug, and disordered intermittent flow. Larger vapour-bubble size at 0-g and low mass flow-rate are generally caused by the larger bubble diameter at the detachment due to forces acting on the bubble at the wall in microgravity (where buoyancy is negligible) and at terrestrial gravity. Fluid velocity has also a significant influence on the shape of Taylor bubbles in intermittent flow. The map of Dukler and co-workers [Colin et al. (1991), and Dukler et al. (1988)], based on void fraction transition criteria, and slightly modified on the basis of current experimental data shows a reasonable prediction capability

Quench front velocity is quite affected by the gravity level, resulting in lower values in microgravity with respect to terrestrial gravity. This effect tends to decrease as the pipe diameter decreases, and to increase as the mass flow rate increases.

ACKNOWLEDGEMENTS

Authors wish to thank Marco Gervasi, Alberto Lattanzi, and Luca Simonetti for their hard work in the experimental work. A special thanks is due to Olivier Minster and Anne Pacros of ESA for their enthusiastic support to the research program, and to Frederic Gay and Christophe Mora of Novespace for their matchless collaboration during the parabolic flights. The work is carried out in the frame of the ESA MAP Contract 14227/02/NL/SH, with the additional financial support of Snecma.

NOMENCLATURE

D tube diameter [m]
g gravitational acceleration [m s^{-2}]
G mass flux [kg $m^{-2}s^{-1}$]
h heat transfer coefficient [$Wm^{-2}K^{-1}$]
j volumetric flux or superficial velocity [m s^{-1}]
p pressure [MPa]
q'' heat flux [W m^{-2}]
Re Reynolds number [-]
s slip ratio [-]
T temperature [^oC]
u velocity [m s^{-1}]
x vapour quality [-]
ΔT subcooling [K]
La Laplace length [m]
D* non-dimensional diameter, D/La, [-]
V* non-dimensional volume [-]
t* non-dimensional time [-]
CHF critical heat flux [Wm^{-2}]
t time [s]

Greek symbols

α void fraction [-]
β packing density [-]

Subscripts

G pertains to the gas (or vapour) phase
in pertains to the inlet conditions
L pertains to the liquid phase
out pertains to the outlet conditions
rew pertaining to rewetting conditions
sub pertaining to subcooled conditions
w wall

REFERENCES

1. H. Ohta, A. Baba and K. Gabriel, Review of existing research on microgravity boiling and two-phase flow. Future experiments on the international space station, *Ann. N.Y. Academy of Sciences*, 974, pp. 410-427, 2002
2. H. Ohta, Heat transfer mechanisms in microgravity flow boiling. Future experiments on the international space station, *Ann. N.Y. Academy of Sciences*, 974, pp. 463-480, 2002
3. P. Di Marco, Review of reduced gravity boiling heat transfer: European research, *J. Japanese Society of Microgravity Applications*, vol. 20, pp. 252-263, 2003
4. J.H. Kim, Review of reduced gravity boiling heat transfer: US research, *J. Japanese Society of Microgravity Applications*, vol. 20, pp. 264-271, 2003
5. H. Ohta, Review of reduced gravity boiling heat transfer: Japanese research, *J. Japanese Society of Microgravity Application*s, vol. 20, pp. 272-285, 2003
6. M. Saito, N. Yamaoka, K. Miyazaki, M. Kinoshita and Y. Abe, Boiling two-phase flow under microgravity, *Nuclear Engineering and Design*, vol. 146, pp. 451-461, 1994
7. Lui, R.K., Kawaji, M., and Ogushi, T., 1994, An experimental investigation of subcooled flow boiling heat transfer under microgravity conditions, 10th International Heat Transfer Conference – Brighton, Vol. 7, pp. 497-502.
8. H. Ohta, H. Fujiyama, K. Inoue, Y. Yamada, S. Ishikura and S. Yoshida, Microgravity flow boiling in a transparent tube, *Proc. 4th ASME-JSME Thermal Engineering Joint Conference*, Lahina, Hawaii, USA, pp. 547–554, 1995
9. H. Ohta, Experiments on microgravity boiling heat transfer by using transparent heaters, *Nuclear Engineering and Design*, vol. 175, pp. 167-180, 1997

10. Y. Ma and J.N. Chung, An experimental study of forced convection boiling in microgravity, *Int. J. Heat Mass Transfer*, vol. 41, pp. 2371-2382, 1998
11. Y. Ma and J.N. Chung, A study of bubble dynamics in reduced gravity forced-convection boiling, *Int. J. Heat Mass Transfer*, vol. 44, pp. 399-415, 2001
12. D.T. Westheimer and G.P. Peterson, Visualization of flow boiling in an annular heat exchanger under microgravity conditions, *J. Thermophysics and Heat Transfer*, vol. 15, n. 3, pp. 333-339, 2001
13. Y. Ma and J.N. Chung, An experimental study of critical heat flux (CHF) in microgravity forced-convection boiling, *Int. J. Multiphase Flow*, vol. 27, pp. 1753-1767, 2001
14. H. Zhang, I. Mudawar and M.M. Hasan, Flow boiling CHF in microgravity, *Int. J. Heat Mass Transfer*, vol. 48, pp. 3107-3118, 2005
15. B.N. Antar and F.G. Collins,Flow boiling during quench in low gravity environment, *Microgravity Science and Technology*, vol. 10, pp. 118-128, 1997
16. C.J. Westbye, M. Kawaji and B.N. Antar, Boiling heat transfer in the quenching of a hot tube under microgravity, *J. Thermophysics Heat Transfer*, vol. 9, pp. 302-307, 1995
17. G.P. Celata, M. Cumo, M. Gervasi and G. Zummo, Flow pattern analysis of flow boiling in microgravity, *Multiphase Science and Technology*, vol. 19, pp. 183-210, 2007
18. C. Colin, J.A. Fabre and A.E. Dukler, Gas-liquid flow at microgravity conditions — I. Dispersed bubble and slug flow, *Int. J. Multiphase Flow*, vol. 17, pp. 533-544, 1991
19. A.E. Dukler, J.A. Fabre, J.B. McQuillen and R. Vernon, Gas-liquid flow at microgravity conditions: flow patterns and their transitions, *Int. J. Multiphase Flow*, vol. 14, 389-400, 1988
20. E.W. Weisstein, Circle packing, From MathWorld, A Wolfram Web Resource, 2006 http://mathworld.wolfram.com/CirclePacking.html
21. E.W. Weisstein, Cubic close packing. From MathWorld, A Wolfram Web Resource, 2006 http://mathworld.wolfram.com/CubicClosePacking.html